Materials Research. 2022; 25:e20220310
DOI: https://doi.org/10.1590/1980-5373-MR-2022-0310

Tribological and Viscoelastic Behaviour of Jute, Prosopis Juliflora Bark, and Kenaf Fibers Reinforced Polyester Hybrid Composites for Engineering Applications

***R. Muthalagu*[a*], *V. Srinivasan*[a], *S. Sathees Kumar*[b], *V. Murali Krishna*[c]**

[a]*Annamalai University, Department of Manufacturing Engineering, Chidambaram, Tamil Nadu, India.*
[b]*Institute of Aeronautical Engineering, Department of Mechanical Engineering, Hyderabad, Telangana, India.*
[c]*B.V. Raju Institute of Technology, Department of Mechanical Engineering, Narsapur, Medak District, Telangana, India.*

Received: July 10, 2022; Revised: October 07, 2022; Accepted: October 09, 2022

Utilizing biomaterials for every conceivable purpose area, such as automobiles, sporting goods, medical, civil, and textile industries, is the aim of the research field. Applications of Natural Fiber (NF) reinforced polymer composites in structural and tribological engineering are rapidly expanding. For the first time in this work, Prosopis juliflora bark and two different types of NF (jute and kenaf) were reinforced with polyester matrix by the hand layup method. The objective of the work is to determine the wear performance and viscoelastic properties of the new hybrid bio-composite. Under dry contact conditions, the tribological performance of the proposed hybrid composite material was evaluated using a range of process parameters, including sliding distance (1000–2000 m), applied load (10–50 N), and sliding velocity (1–5 m/s). The wear behaviour of the fabricated NF composite was greatly enhanced (17.5 x10^{-8} mm^3 /N-mm) by the higher composition of kenaf fibers has been observed. The dynamic mechanical analysis (DMA) showed that the manufactured composites had high storage modulus (4.1 GPa) and loss modulus (3.8 GPA). SEM was used to investigate and propose a potential wear mechanism for the developed composites by evaluating the exterior geomorphology of samples after wear tests. AFM provided details on the fiber surface properties of hybrid composites.

Keywords: *DMA, juliflora, kenaf, Polyester, Wear.*

1. Introduction

Several applications of NF-reinforced composite materials have been the focus of intense research over the last ten years. Polymers can be reinforced with abundant natural fibers to create robust and lightweight materials. Natural fibers derived from plants are beginning to appear in industrial settings, such as the automotive and household goods industry segments. Fiber composites have been used in structural and infrastructure applications to rebuild old structures, bridges, and other structures, particularly those in marine or corrosive environments[1-3]. Furthermore, NF composites have been used in structures subjected to a variety of loads and environmental conditions. Examples include wind turbines, bridges, wooden beams, roofs, floating river crossings, structural portal frames, monocoque fiber composite trusses, truss systems, and railway sidings for transportable shelters[4-9]. Because of the demand for more environmentally friendly substances, NF composites are regaining the attention that was previously diverted to synthetic products. The use of fiber-reinforced clay for elements and pots was the first documented application of natural fiber composites[10]. Synthetic fibers dominated early fiber composite research and development. Despite their outstanding performance, synthetic fiber composites made of glass, carbon, and aramid fibers are less biodegradable and derived from non-renewable resources. In the automotive industry, NFRP composites are used to make headliners, door panels, dashboards, interior car parts, and package trays[11,12]. Other products, such as Sliding panels, linkages, bearings, and bushings are also gaining increased application[13]. Because of their wide range of industrial and commercial applications, NF composites are occasionally subjected to varying tribological loading conditions, which expose the component to a variety of wear mechanisms such as abrasive, adhesive, and sliding wear. It is critical to assess and study the tribological performance of the generated composites to make them more useful in many technical fields. Several variables affect the wear and friction of NF composites, including the type of reinforcement, fiber treatment, fiber positioning, waterless and saturated interaction conditions,

*e-mail: muthalagurr@gmail.com

and fiber weight percentage[14,15]. According to previous research[16,17], bio-composites performed better in terms of wear under wet contact conditions than they did under dry contact conditions. Numerous researchers have contributed to the tribological study of NF composites. The inclusion of matrix reinforcement to the fibers has improved the NF composites' wear rate. According to Bajpai et al.[18], a sisal/polypropylene composite demonstrated wear and frictional behaviour under a variety of process conditions such as applied loads (10–30 N), sliding velocity (1-3 m/s), and a constant sliding distance of 2000 m. The researchers concluded that incorporating 30% sisal fiber increased the wear resistance of the produced composite over plain polypropylene. Natural fibers in the form of fibers, such as Abutilon Indicum (AI), Prosopis juliflora (PJ), and Tapsi (T), were considered in the latest study. Composites were developed for three distinct fibers. The created composite samples were subjected to wear tests with varied process constraints, such as sliding velocity and applied load, at distances of up to 3000m. The polyester-reinforced PJ composite sample has a higher SWR according to the wear test findings than the other two composite samples[19]. The mechanical features and thermal stability of untreated and chemically treated coconut fiber (Cf), banana fiber (Bf), and Prosopis juliflora bark (PJb) reinforced epoxy hybrid mixtures were studied by S. Sathees Kumar and V. Mugesh Raja. The mechanical behaviour of treated and untreated composite specimens was contrasted. Alkali-treated composite specimens have exclusive mechanical characteristics compared to raw fiber composites[20]. The performance of polymer composites has improved recently, which has drawn a lot of attention to studies on kenaf-reinforced polymer composites (KFPC). The possibility of using kenaf fiber in place of synthetic fibers has drawn the attention of numerous researchers[21]. KFPC had better wear qualities than other polymer composites reinforced with sugarcane, oil palm, and jute according to research conducted by Chin and Yousif[22]. In comparison to the other natural fibers examined, they concluded that kenaf fibers offered an assuring alternative to synthetic fibers for wear applications. Even though numerous studies have been conducted on improving the qualities of NF-reinforced polymer composites, their performance occasionally falls short of expectations or has only mderate improvements in terms of their properties. When compared to synthetic fiber-reinforced polymer composites, the variety of NF-reinforced polymer composite qualities is still inadequate. This is brought on by natural fibers' lower mechanical strength as compared to synthetic fibers and their incompatibility with the polymer interface. Heckadka et al.[23] investigated the two-body wear behaviour of natural fiber reinforced composites. Natural fibers such as Polyalthia longifolia, Mangifera indica, and jute were used as reinforcements with an epoxy matrix. A load of wear tests was taken from 1 kg to 4 kg. From the outcomes, 2kg has attained the optimal wear rate. Numerous modifications to NF themselves have been made to improve the performance of NF/polymer composites. Many previous studies report the use of dissimilar fibers to improve the properties of NF composites. In this work, for the first time, attention was paid to the tribological characteristics of hybrid composites comprised of one plant bark powder (Prosopis juliflora bark) and two plant fibers (jute and kenaf). Earlier in NF composite work, the maximum load utilised was 40 N for the wear test. In this study, wear tests were subjected to a maximum load of 50 N. Furthermore, DMA was carried out to identify the viscoelastic properties of hybrid composites. also identified the morphological images of worn surfaces through SEM.

2. Materials and Methods

Jute fiber, Prosopis juliflora bark, and kenaf fiber were used in this experiment's creation. In the Ramanathapuram district of Tamil Nadu, India, juliflora bark, kenaf, and jute fibers are gathered as remnants. Methyl ethyl ketone peroxide is purchased from M/s. Global Scientific Ltd. in Coimbatore, Tamil Nadu, India as a catalyst and cobalt naphthenate acts as an accelerator. Unsaturated terephthalic polyester resin with a pre-accelerated structure, marketed as Denverpoly 754 by Royal Polymeros, was the polymer used in this work improvement. 2 to 3 cc of resin was used, and the catalyst contained 2% cobalt naphthenate

2.1. The abstraction treats fibers

2.1.1. Bark from Juliflora plant

The juliflora plant has flexible branches with long, sharp thorns and a twisted stalk. The roots may grow in a variety of soil types, including saline, sandy, rocky, and alkaline, and they can reach large depths in the ground. It occurs in dry or semiarid areas all over the planet[24]. This plant's juliflora served as a resource for NF. The size of the bark is around 20mm x 10mm. The outer layer was kept for later separation of the bark, while the inner layer was removed and discarded. Table 1 represents the physical characteristics of NF.

Table 1. Chemical constituents and Physical properties of Natural Fibers.

Physical Properties	Jute fiber	Kenaf fiber	juliflora bark	References
Cellulose (%)	61.2	44.4	61-65	20,25,26
lignin (%)	13.7	20.1	15-18	20,25,26
Hemicellulose (%)	23.2	21.5-23	32.1- 32.83	20,25,26
Moisture (%)	7.5	7.27-7.67	4.64 -7.3	20,26,27
Ash	1.0	4.6	1.13	20,26,27
Density (g/cm^3)	1.3	1.2	0.58 - 0.73	20,25,26
Fiber length (cm)	2 - 60	4 - 30	Bark Thickness (mm) 1.09-2.53	20,25,26
Fiber Dia. (μm)	17 - 20	55 - 60	52x10^3 - 60x10^3	20,25,26

2.1.2. Fibers from the jute plant

Jute fibers are trimmed to a length of 4 to 5 cm and then cleaned in distilled water. They took 3 to 4 hours to dry. The fibers are then immersed in a 5% concentrated NaOH liquid for 24 hours at 32°C before being cleaned with deionized water to remove any remaining NaOH that has adhered to the fibers. The fibers are then allowed to dry for 7 to 8 hours at room temperature.

2.1.3. Fibers from the kenaf plant

Water retting was used to finish the process of removing the fiber from the Kenaf plant. For 26 days, the kenaf plant's stems were submerged in water and held in place by aquatic plants. Finally, the filaments were properly cleaned, dried in the shade, and stored in preparation for further use[3,28].

2.1.4. Alkaline treatment of natural fibers

When combined with other compound changes, alkaline treatment, an NF external treatment, can also be exploited as a pre-treatment. These processes were initially performed to increase the fiber's attraction to dye and shine[29]. Thus, it was found that alkalization as well has a favourable impact on the mechanical features of composites reinforced with fibers, leading to noticeable improvements in the interfacial execution[30]. An alkali treatment was used to complete the surface treatment of the strands to raise their quality. The corresponding weight ratio of the strands was rinsed in distilled water, dried at room temperature, and then engrossed in 5% NaOH concentrates for 5 hours with physical mixing every 20 minutes. The minimal-thick polyester resin of profitable-grade Methyl Ethyl Ketone Peroxide (MEEKP) and Denverpoly 754 is used as a matrix material to create various gel memories from 120 min. to 180 min.

2.1.5. Preparation of composite

The Prosopis Juliflora barks that had been collected were divided into 4-5 thorough washings in clean water to remove pollutants like dust. Fresh raw Prosopis Juliflora barks were exposed to the light for a week before being dried for an hour at about 105°C in the oven. These were then ground into bark powder using a grinder and sieved to a particle size of 300 mm, then kept in plastic bottles. The powdered Prosopis Juliflora bark was combined with the dried jute and kenaf fibers, which had been cut into 3 to 4 mm pieces. The two fibers and powder combined sped up the alkaline treatment. The hand layup process starts when the alkaline treatment has finished.

2.1.6. Fabrication of composite samples

The development of natural fiber-reinforced polyester composites used the hand lay-up moulding technique. A 100 x 100 x 10 mm^3 mould was used for the creation of unidirectional oriented composites. To avoid adhesion between the mould and the composites and to aid in the removal of the manufactured composites, the mould surface was coated with a mould release agent. Table 2 lists the composite's compositional variations and designations. The 10% polyester resin and 1% hardener were first thoroughly combined at room temperature before being put as a layer into the mould. After the resin layer, the fiber and powder mixture were positioned horizontally in the mould. Similar to this, polyester resin was used, and the initial layer was then covered with a mixture of powdered fibers. Four layers of the composite were made in total using the aforementioned method. A roller was run over the manufactured composite to enhance the resin absorption and reduce the creation of voids. The fabrication of samples as shown in Figure 1

Table 2. Composition and designation of hybrid composite samples.

Natural fibers (wt %)			Designation of samples
Jute fiber	Juliflora bark powder	Kenaf fiber	
50	**40**	**10**	**A1**
50	**30**	**20**	**B2**
50	**25**	**25**	**C3**
50	**20**	**30**	**D4**
50	**10**	**40**	**E5**

2.1.7. Wear test

As per ASTM G99-95, pin-on-disc tribometer tests for friction and wear were performed (DUCOM India, TR-20LE-PHM 400) as per ASTM G99-95. The counter face of the tribometer was made of case-hardened EN 31steel (HRC 60)[31].

2.1.8. Dynamic Mechanical Analysis (DMA)

Dynamic mechanical properties of hybrid composites were examined as an operation of temperature (20-100 °C) using a DM Analyzer (TA 2980) set up with a twin cantilever bending fixedness at a frequency of 1 Hz and a constant heat up rate of 5 °C/min.

2.1.9. Atomic force microscope (AFM)

A typical atomic force microscope can take photos at a resolution of 256 x 256 pixels at scan rates of 10–20 m/s (Digital Instruments, Santa Barbara, CA).

2.1.10. Surface Roughness test

The composites' arithmetic mean surface roughness (Ra) was measured using a compact surface roughness tester (Model: MITUTOYO SJ-210 Series). Figure 2 depicts the experimental test setup. On the worn-out surface, the traceability distance was set to 2.5 mm. The surface texture value for each sample was determined twice at different locations, and the average reading was calculated as the Ra of the corresponding sample.

3. Experimental Work

3.1. Pin–on–disc tribometer setup

The friction force, temperature, time, and time/revolutions monitoring are also displayed on the tribometer's numerous digital display indicators. As the rotation begins, the specimen in the specimen holder rubs against the steel counter face. A pulley mechanism is also used to transfer the dead weight. Figure 2 illustrates an image of the experimental setup. The silicon carbide (SiC) abrasive paper adhered to the cylindrical-shaped carbon steel spinning disc and the pin-

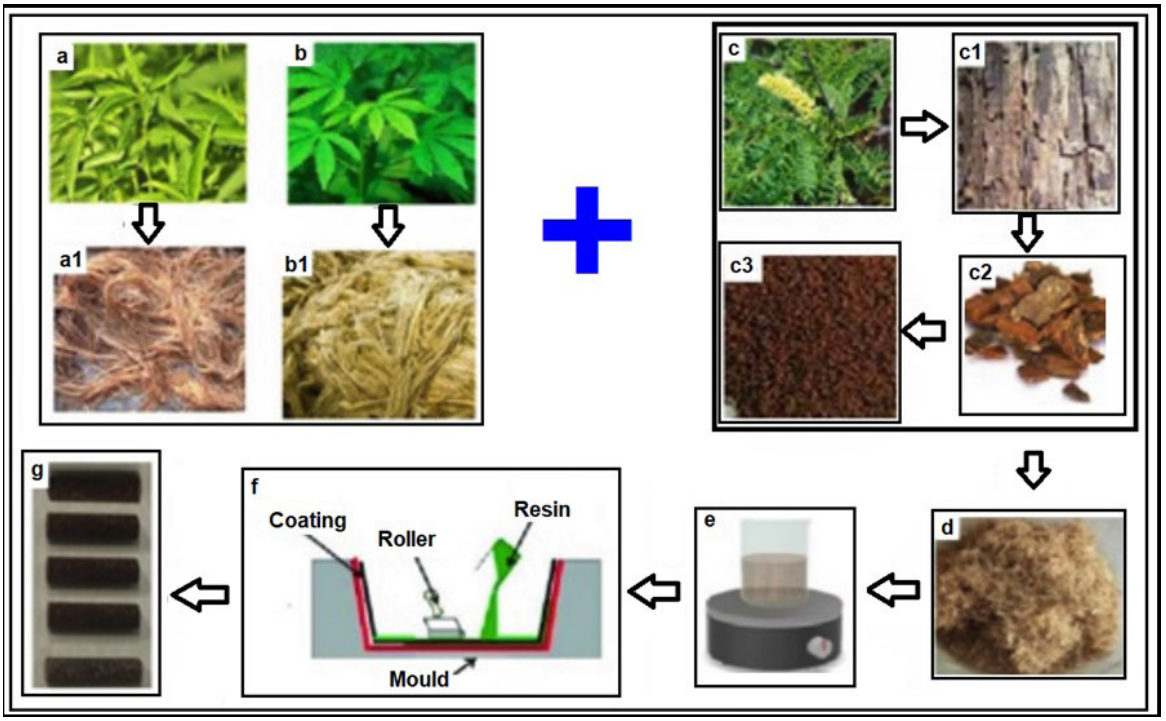

Figure 1. Fabrication process of hybrid composite samples. a. Jute plant, a1. Jute fibers, b. Kenaf plant, b1. Kenaf fibers, c. Juliflora plant, c1. Juliflora bark on the plant, c2. Bark removed from Plant, c3. Bark powder, d. Fibers and powder mixture, e. Alkaline treatment, f. Hand lay-up process g. f abricated composite samples.

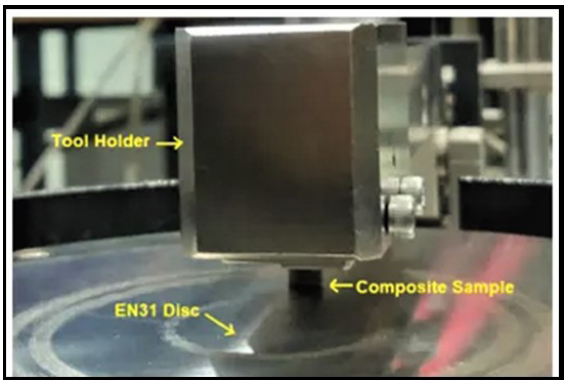

Figure 2. Tribometer setup.

shaped mixture samples with a diameter of 8 mm and an extent of 20 mm were slid across it. Following each experiment, cotton was used to wipe the plate and specimen with acetone. The samples were moved against the counter face while maintaining their natural orientation in the direction of the hybrid composite fibers. With a track diameter of 100 mm and dry sliding circumstances (1000 – 2000m), the test was run for 2000 s while controlling various factors such as sliding speed (1-5m/s) and applied weight (10-50N).

The Shimadzu (AUW220D) electronic balance was used to quantify each sample's weight loss from wear before and after the test with an accuracy of 0.1 mg. The wear volume loss was then computed by dividing the weight loss by the specific composite density. In the Winducom software, the frictional forces and frictional coefficients of the samples were created, recorded, and the average frictional coefficient was calculated. The average of three repetitions for each sample was used to calculate all the wear and friction data.

4. Results and Discussion

4.1. Co-efficient of frictional force

A range of sliding speeds (1, 3, and 5 m/s), applied loads (10 to 50 N), and sliding times were used in experiments to determine the friction force (960 sec, 1440 sec, and 1920 sec). For all kinds of the created mixtures at various weights and a stable velocity of 3 m/s, the frictional force was mapped versus the sliding time. For all the fabricated samples, increasing the applied load from 10 to 50 N exhibited expanding trends in the frictional force. The frictional coefficient at various loads is revealed in Figure 3, Figure 4, and Figure 5.

A1 reached its extreme friction force of 7.43 N with a load of 10 N and a sliding velocity of 3 m/s. The B2 composite and C3 exhibited friction forces of 6.62 N and 6.43 N, respectively. D4 and E5 both achieved a friction force of 5.28 and 5.42 N, respectively. Furthermore, A1 reached a high friction force of 38.73 N at a load of 30 N and a sliding velocity of 3 m/s as compared to the friction force of E5 (22.74 N). B2 and C3 each had friction forces of 32.45 N and 28.48 N, respectively. D4 generated a 24.78 N friction force. The frictional coefficient at a sliding velocity of 1 m/s is shown in Figure 6. B2 and C3 achieved maximum frictional coefficients of 0.78 and 0.62, respectively, while

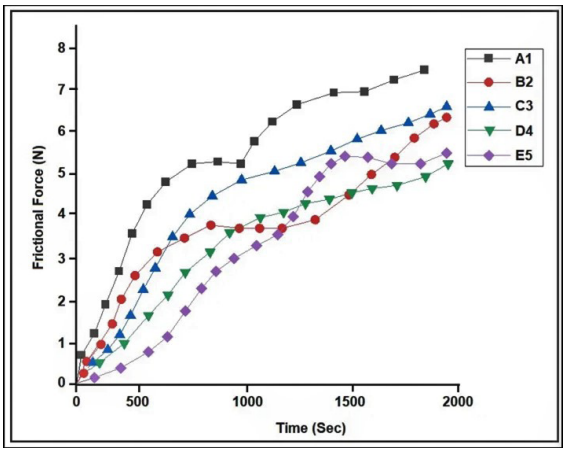

Figure 3. Friction force at 10N Load and 3 m/s sliding velocity.

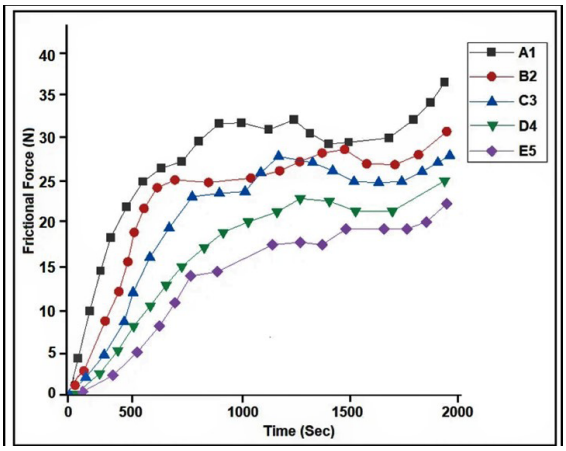

Figure 4. Friction force at 30N Load and 3 m/s sliding velocity.

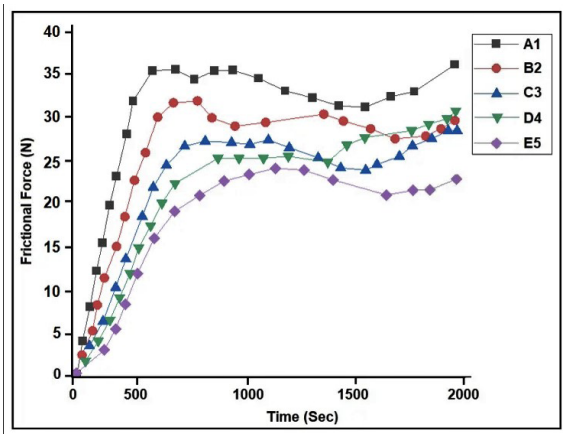

Figure 5. Friction force at 50N Load and 3 m/s sliding velocity.

A1 reached a maximum of 0.84. The frictional coefficients for D4 and E5 were 0.54 and 0.48, respectively.

A1 reached its maximum friction force of 38.32 N with a load of 50 N and a sliding velocity of 3 m/s. This might

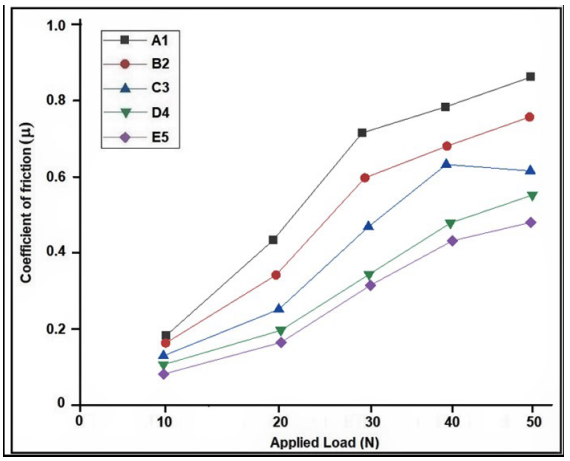

Figure 6. Coefficient of friction at 1m/s sliding velocity.

be because there are not as many raw fillers in the mixture, which tends to reduce the amount of interfacial adhesion among the filler-resinous zones. Due to the poor surface hardness, it was found that the material removal rate was higher in the resinous regions compared to the filler regions[32]. As a result, different polymeric wear must be considered as a function of load condition, sliding speed, heating rate, and total distance moved. The exterior temperature has a major impact on polymer wear. Thermal deformation may cause the rate of wear to increase. In general, a thinner soft layer results in less wear. The experimental results also showed that as the velocity of sliding and normal load increased, so did the temperature of the specimen. The coefficient of friction rises with increasing sliding speed and normal load distribution, as shown in Figure 7 and Figure 8. The weight loss of all polyester composite specimens increased as the normal load was raised at the same sliding distance. The A1 composite has the highest friction force of all the developed composites. Owing to the irregular exterior of the jute fiber and 40% of the juliflora powder, the interfacial interaction among the fiber/matrix bonding of the hybrid polyester mixture increased to its maximum wettability. The frictional coefficient of hybrid composites was shown in Figure 7. B2 and C3 achieved 0.48 and 0.32, respectively, while A1 obtained the highest rating of 0.57. Additionally, the frictional coefficients for D4 and E5 were 0.18 and 0.84, respectively. By incorporating an additional proportion of kenaf fiber, composites B2 and C3's frictional force was also increased. The interfacial interaction among the fiber/matrix interfaces is also strengthened by the low amount of juliflora powder and the high percentage of kenaf fibers. The B2 composite and C3 had friction forces of 32.65 N and 27.49 N, respectively. D4 and E5 achieved friction forces of 25.12, 23.42 N, and 26.76 N, respectively. In the matrix, the fillers were gathered. The filler and the matrix's bonding strength were weakened as a result. Greater shear force at the interface caused by higher filler content caused more filler to leak out of the composite. With increased sliding distance, a trend toward steady decline was seen. In comparison to composites made with high wt.% kenaf filler, this friction coefficient was found to be lower. Because of improved

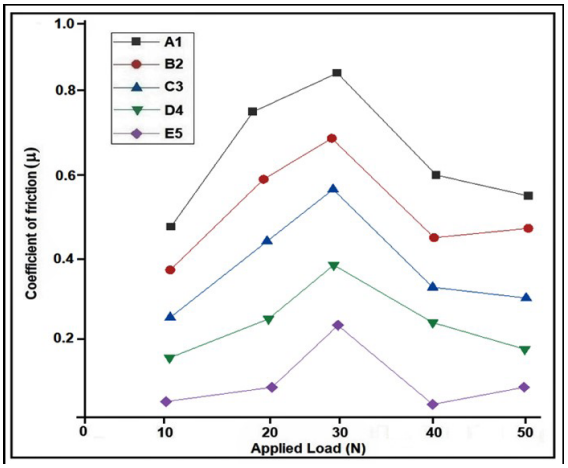

Figure 7. Coefficient of friction at 3m/s sliding velocity.

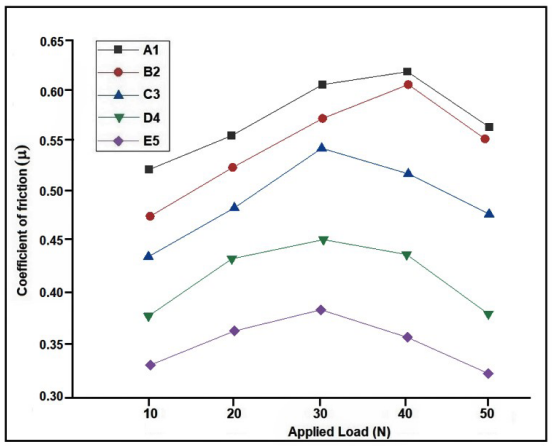

Figure 8. Coefficient of friction at 5m/s sliding velocity.

interfacial interaction between the filler and matrix, it was discovered that the frictional coefficients of each sample for all sliding velocities varied less.

Because only the even, glassy deposit of polyester is in touch with the sliding counter face, there is no fiber interaction, which reduces the frictional coefficient. Friction force and thus frictional co-efficient are determined by the interaction between the composite rubbing surface and the counter face. It has been determined that the main mechanisms influencing friction are adhesion and deformation. On a rough surface, deformation predominates, whereas adhesion affects a smooth surface[33,34]. The frictional coefficient of hybrid composites was shown in Figure 8. B2 and C3 achieved 0.56 and 0.47, respectively, while A1 obtained the highest value of 0.58. Moreover, the frictional coefficients for D4 and E5 were 0.37 and 0.33, respectively. Overall, processed kenaf had a lower friction coefficient than a higher wt.% of other hybrid composites. This might be explained by stronger interfacial bonds between the matrix and filler[25,35]. The bonding strength reduces the amount of material removed, reduces the friction force, and increases wear resistance. The amount of soft wreckage accumulated between fibers was relatively higher on rubbing surfaces. The increase in the 30 N load contributes to the previously occurring wear process. This increase in load causes both an increase in the temperature of the sliding interface, which was also observed, and a greater impact of mating surface irregularities on fibers particularly the coefficient of friction. In the current study, it was noted that the rough surface of the composite sample smoothed out after a period of sliding. This resulted from a thin polymer film building up on the composite's rubbing surface. After some rubbing, the frictional coefficient was reduced as a result of the deposition of the polymer film.

4.2. Wear rate

Figure 9 demonstrates that for all the produced composites, the wear rate increases as the sliding velocity increases. First, for all sliding velocities, the wear rate reduced as the load changed from 10 to 30 N, but rose or remained stable as the load altered from 30 to 50 N. This suggests that weight loss of up to 30 N of applied force is relatively minimal. With an increase in applied stress beyond 30 N, weight loss has grown considerably more quickly. At all operational circumstances for load, sliding distance, and sliding velocity, the B2 sample produced the highest rate of wear of19.3 $x10^{-8}$ mm^3/N-mm. The wear rate of composites is found to rise with rising load and sliding velocity in prior studies[26,36,37]. According to Figure 9, A1 had a wear rate of 17.8 $x10^{-8}$ mm^3/N-mm at 10 N applied stress and 1 m/s sliding velocity. The composites' extensive fillers and expanding real contact area may be the causes of this. The wear rates for C3 and D4 were 13.7 $x10^{-8}$ mm^3/N-mm and 12.8 $x10^{-8}$ mm^3/N-mm respectively. The E5 had a wear rate of 4.1 $x10^{-8}$ mm^3/N-mm. The significant filler component of the composites was essential for the material elimination method, and the fillers subsequently caused the wear. The existence of matrix sections throughout wear out was steadily decreased by enhancing the filler substance and surface rigidity levels, which would drop the thermomechanical loading. At low velocity (1 m/s), the specific wear was initially high for all compositions, but as velocity increased, the specific wear gradually dropped to 5 m/s. The wear rate decreased slightly for all samples as the velocity enhanced from 1 to 3 m/s, and then it barely decreased until the velocity exceeded 5 m/s. A low wear rate was seen at higher sliding velocities because more fibers were exposed to abrasion from the sliding disc, which increased the jute resistance. To facilitate the cutting of fibers, more energy was needed. As a result, the wear rate declines as the sliding velocity rises[38]. A rise in load caused the interface hotness to rise because of friction between the composite sample and the disc. The composite sample becomes brittle due to friction at the contact and gradually fails the fibers and parts. Because it may also serve as a lubricant, the wear rate decreases with increasing load as a result of the creation of a thin layer by the fibers[39]. The variance in the wear rate of the composite sample under the same progression constraints is caused by the behaviour of the NF. This shows that the wear implementations depend on the natural fibers' uniqueness as well as their matrix. The reduced wear characteristics of a composite are the result of insufficient bonding. Heat generation, which is again influenced by the applied loads,

causes periodic fluctuations in the temperature of the fiber matrix contact. The wear rate percentage of hybrid composite samples such as A1, B2, C3, and D4 achieved 76.9%, 78.7%, 70.07%, and 67.9% respectively compared with the E5 sample.

In Figure 10, the wear rate dropped as the load improved from 10 to 30 N, but it increased whenever the load increased from 30 to 50 N for the A1 sample. At a 10 N load and 1 m/s sliding velocity, A1 and B2 samples attained a wear rate of 44.7 x10^{-8} mm^3/N-mm and 33.3 x 10^{-8} mm^3 /N-mm, respectively. C3 and D4 also demonstrated wear behaviours of 17.7 x 10^{-8} mm^3/N-mm and 14.3 x 10-8 mm^3/N-mm, respectively. Additionally, the E5 composite obtained a minimum wear rate of 11.1x10^{-8} mm^3 /N-mm. This result could be an enhancement in the real interaction area as well as a progressive increase in the filler content in composites. This can be the point at which the resinous region has lost the most material and has less wear resistance. The wear rate percentage of hybrid composite samples such as A1, B2, C3, and D4 achieved 75.1%, 66.6%, 37.2%, and 22.3% respectively compared with the E5 sample. During the studies, minute particles leached out of the material; this may have created a back coating on the counter; This resulted in three distinct contact mechanisms. It was reported that there has been a large variation in the attributes of different mixtures of the created composites based on the mechanical attributes of these composites as stated elsewhere[40]. The wear performance of these composites would undoubtedly be influenced by this. These differences are caused by variations in the properties, components, interactions, and compatibility of numerous natural fibers with the polyester polymer matrix. Figure 11. As the load varied from 10 to 30 N, the wear rate diminished, but further augmentation in the load varied from 30 - 50 N at 5 m/s sliding velocities improved the wear rate of A1 (56.7x 10^{-8} mm^3 /N-mm) hybrid composite sample. Due to the low surface hardness, it was found that the material removal rate was higher in the resinous regions than in the filler regions. B2, C3, D4 and E5 achieved the wear rate of 43.3 x 10^{-8} mm^3 /N-mm, 31.4 x10^{-8} mm^3 /N-mm, 22.6 x10^{-8} mm^3 /N-mm and 17.5 x10^{-8} mm^3 /N-mm respectively. The wear rate findings in the four samples appear to differ substantially between samples. This might be a result of the test's initial uneven surface wear and lower filler content. Continuous interactions between a hard surface and a smooth composite pin were linked to the production of wear debris, which tended to form a thick back film on the worn exterior and slide among the molecular layers. This could have been caused by intense thermomechanical loading among the faces. In the case of tribo-properties, however, both friction and wear effectiveness decreased exclusively as fiber orientation continued to increase. Wear decreased under severe loading conditions, confirming the composite's suitability as a dry bearing for rough operating conditions. It showed the greatest update to its reflective and mechanical properties[41]. In the experiments, the fillers experienced low shear opposition at the counter face roughness zone, which significantly reduced material removal. At the extreme weight content of juliflora bark powder composites, both the fillers and resinous regions were worn out. Then the fillers and the resinous region were directly affected by the sliding force, which reduced the wear rate of hybrid composite samples. The wear rate percentage of hybrid composite samples such as A1, B2, C3, and D4 achieved 69.13%, 59.58%, 44.26%, and 22.56% respectively compared with the E5 sample.

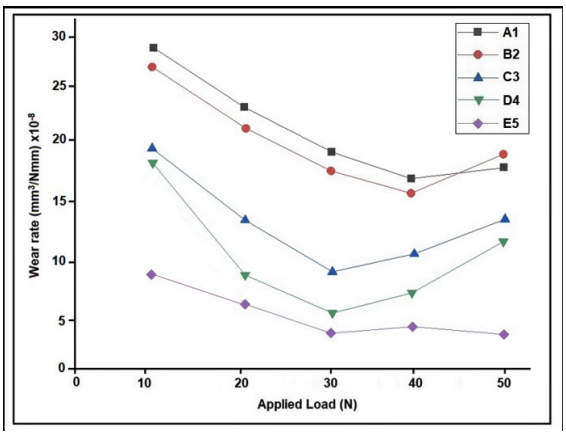

Figure 9. Wear rate Vs applied load at 1m/s sliding velocity.

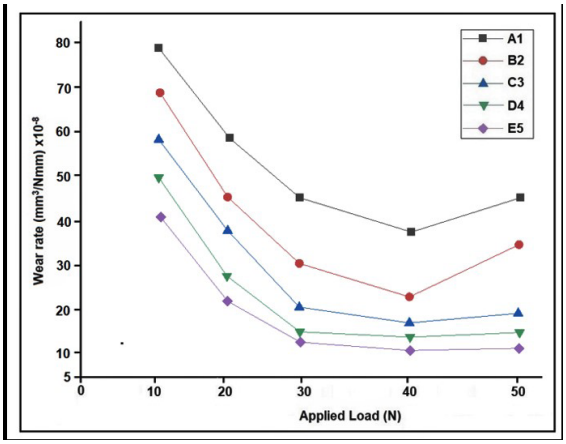

Figure 10. Wear rate Vs applied load at 3m/s sliding velocity.

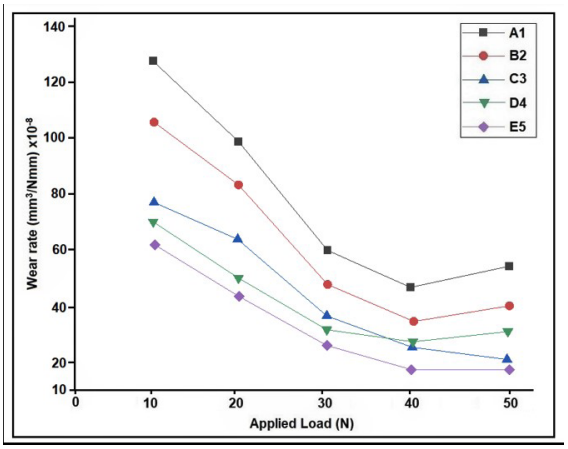

Figure 11. Wear rate Vs applied load at 5m/s sliding velocity.

4.3. Characteristics of damping

DMA aids in identifying the serenity and phase transformation activities in various combinations of material behaviours. Additionally, it is a more effective and efficient technique to research the tranquilities in neat polymers and polymers that comprise fiber. The relevant tan D (Material loss factor) and stiffness of clean and fiber-amalgamated mixtures are also determined using this method for a range of applications[13,14]. This demonstrates that chemically modified fiber-reinforced mixtures have higher E′ rates and higher flexural modulus. The alkaline treated fiber composite sample E5's E′ value increased. The dynamic mechanical tests revealed a higher value of E′ (4.1 GPa) due to improved intermolecular interactions in hydroxyl groups. This Figure 12. shows a stronger bond between the matrix and the kenaf fibers with changed surfaces. These DMA results demonstrated that silane-treated fibers increased the thermal durability of composites[40].

It should be noted that the composite sample E5, which was reinforced with jute, kenaf fibers, and Juliflora bark powder, exhibited E' of 4.1 GPa at 136° C. Combining jute, or E5, with kenaf reinforcement increased the storage modulus. As seen in the storage modulus curves, the loss modulus (E") decreased with higher weight fractions of fibers in the polyester matrix. As a result, the temperature linked to the maximum E was lowered by the inclusion of these fibers. With Tg happening at lower temperatures, the viscous stiffness decreases as the temperature drops. The data also show a relaxation peak in the 100 to 150 °C hotness range. The existence of this peak, according to Mohanty et al.[41], can be explained by structural relaxation, which is attributable to the mobility of polymer chains in the polymer matrix's crystalline phase due to defect reorientation. The pure polyester resin exhibits increased structural damping as expected because the parameter tan D is linked to damping or internal friction[32]. Fiber addition reduced damping, which would have been caused by load transmission from the polyester matrix to the kenaf fibers. Furthermore, as a result of the addition of kenaf fibers to the polyester matrix, the temperature at which the greatest tan D occurred was shifted below. The glass transition temperature, Tg, was found to have peaks in Figure 12, which are shown in each curve. When kenaf fibers were heavier in polyester composites, there was a drop in the damping factor. This has to do with how the matrix and kenaf fiber interact, which lessens the polyester's capacity to crystallize.

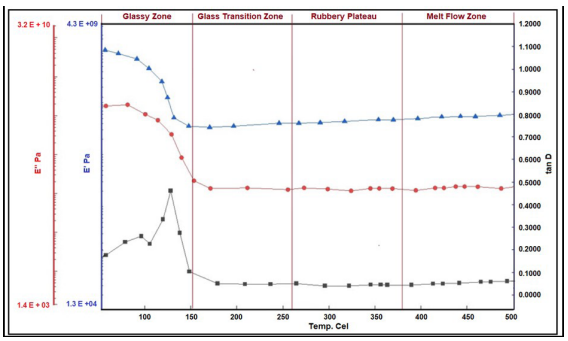

Figure 12. Damping characteristics of sample E5.

4.4. SEM micrographs

Figure 13 shows SEM images of alkaline-treated hybrid composites. SEM micrograph at 3 m/s sliding can support a load and speed rate of 50 N. Broken Fiber and microfracture are evident at greater loads. as seen in the ACE1 composite SEM image. According to Chin and Yousif[22], increasing the load caused the fiber to debond caused by thermomechanical loading, which made the fiber/matrix interfacial connection weaker and made it easier for material to be removed from the polymer matrix. SEM micrographs of the C3 mixture only exhibited less breakage in the fibers, which contributed to the lowest wear rate among the other produced (A1 and B2) composites. Due to the lower proportion of palm fibers, microscopic observation of the A1 composite material following wear testing exhibited microcracking and broken fibers. Typically, palm fibers have strong ductile capabilities. However, the B2 sample exhibits microfracture and broken fibers because jute fibers are brittle. Large debonding and wear debris are seen in A1, which in turn leads to a faster rate of material removal. A larger applied load denotes a fiber fracture. The hydrophobic alanine and glycine compounds, which have a higher propensity for forming a strong link with the polymer matrix, were activated by the alkaline treatment of the fiber, which also removed the sericin component. It was discovered through the SEM examination that the broken fibers and microfractures were what caused the two composite samples to fail. When compared to other samples, the texture of the A1 sample, as shown in Figure 13, had many more waxes and impurities. There is a contaminant accumulation along the fiber, which can be seen. The removal of hemicellulose and pectin from samples C3, D4, and E5 reveals a clear exterior and a rough texture. Additionally, the D4 composite sample had poor adhesion B2 and more broken fibers and microfractures than usual. Large debonding and wear debris are observed in C3 and D4, implying a fiber fracture and a higher rate of material loss, respectively, when combined with a higher applied load. The fiber cell debonding on the sliding surface is depicted in C3. Microfractures were produced on the worn exterior at a relatively elevated applied load in Figure 13. (D4) (50 N). Microfractures lead to material failure and speed up wear at greater applied loads. Under harsh conditions (greater load and/or velocity), microfractures predominate as a wear mechanism[27]. In addition, the worn surface has microfracture from the pin adhering to the counter face. Cracks arise when adhesion transfers a portion of the composite to the counter face. Due to excessive pressure in some areas, fragile polyester resin has separated, causing the plastic to distort and debris to be produced.

In Figure 13. E5 the presence of the kenaf fiber (40%) ends on the worn surface demonstrates strong bonding and an absence of pull-out between the fiber and matrix. The polyester layer is created by debris conversion from resinous zones and covers the cross-section of the fibers, which inhibits material exclusion from the mixture exterior and lowers the wear rate. The wear rate is considerable at 50 N applied load, and it decreases at elevated applied loads, according to the results as shown in Figure 13.E5. As a result, removing or separating fibers from the matrix is practically impossible and tends to slow wear[42-44]. The impact of fiber

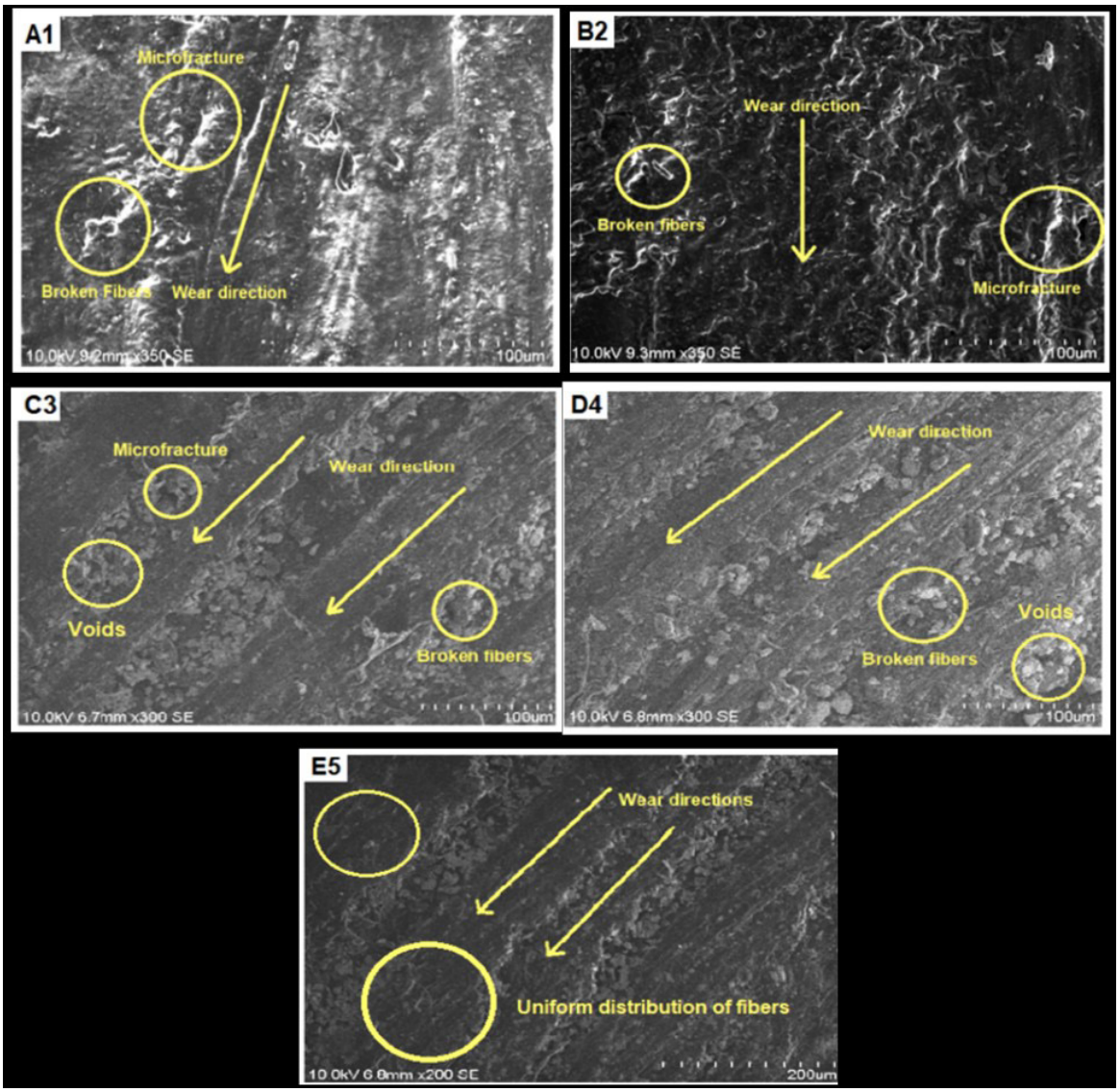

Figure 13. SEM morphologies for worn-out surfaces of hybrid samples.

direction on wear appears to be more significant, as normal fiber orientation generated the lowest wear despite having the highest frictional force[45]. The study findings show the significance of fiber orientation in composite sliding wear. Additionally, the fiber orientation has a significant impact on how the composites wear, with normal alignment exhibiting the least wear rate when compared to neat polyester and other fiber combinations since the fiber ends are exposed to the sliding counter face. Alkaline treatments are used to have a positive impact on fiber morphology at higher weight proportions of kenaf fibers (D4 and E5), resulting in a uniform distribution of impurities.

4.5. Surface topographical analysis for hybrid composites

The topographic images created by AFM after the alkali treatment showed notable changes in fiber surface form. Atomic force microscopy (AFM) may generate high-resolution pictures of the sample exterior in both 2-D and 3-D without significantly affecting the surface of the fibers[46]. Topographical AFM pictures of the natural fiber composition of the E5 sample are shown in Figure 14. The average exterior roughness (Ra) of composites was found to be 41.089 nm, indicating the occurrence of contamination and amorphous lignin on the exterior of the natural fibers. Other surface characteristics such as skewness (Rsk), RMS roughness (Rq), kurtosis (Rku), the extreme height of the contour (Rt), and average full height of the contour (Rz), are -1.224 nm, 61.523 nm, 332.658 nm, 299.057 nm, and 7.178 nm correspondingly, that confirm these findings. In an attempt to optimise the different surface morphology, surface modifications are required for the potential utilisation of natural fiber composites as a strengthening substance in polyester composites.

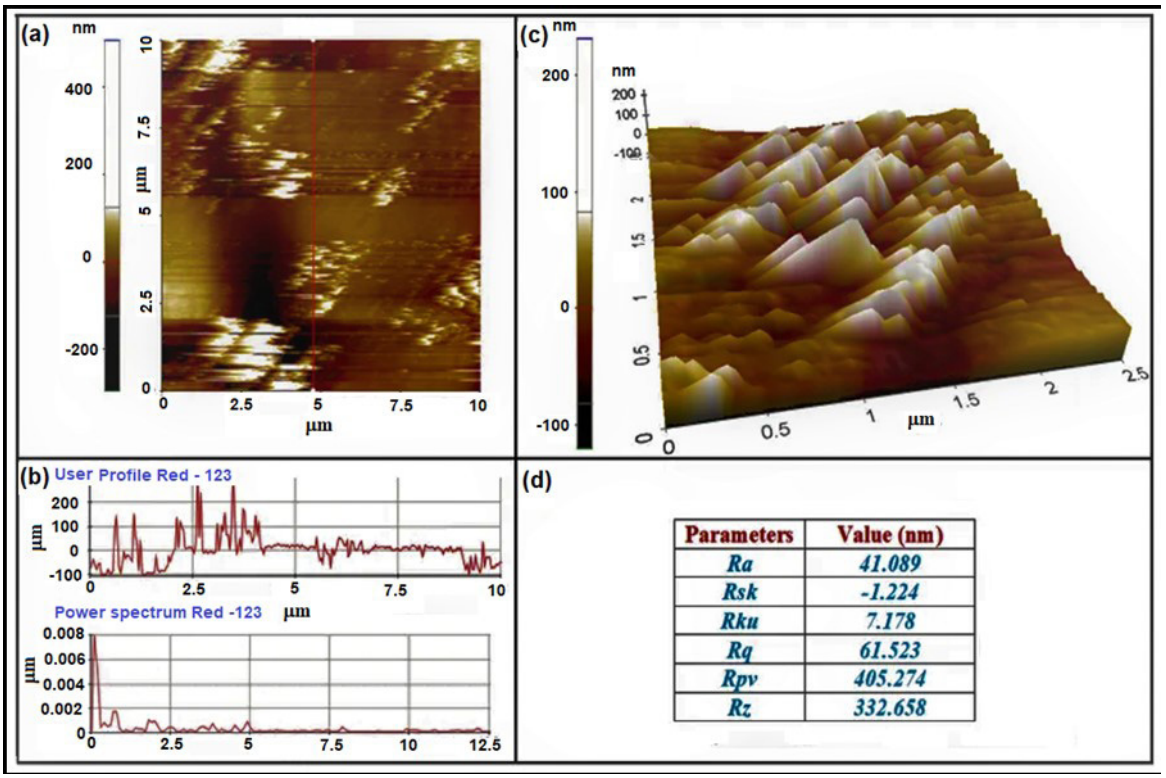

Figure 14. (a) Roughness Surface Texture, (b) 2-D Line Diagram for Roughness measurement of NF, (c) 3-D Roughness Surface Texture, and (d) Roughness Parameters.

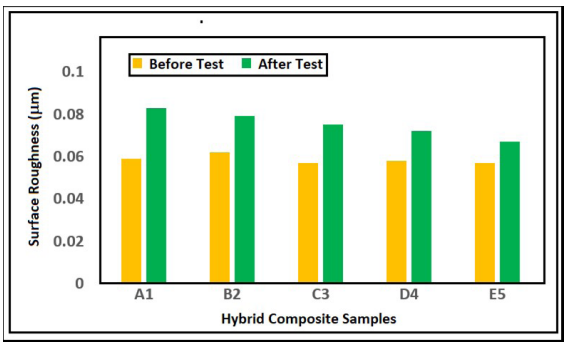

Figure 15. Mean surface roughness of hybrid composite samples before and after wear test.

4.6. Effect of sliding on surface roughness

It is well known that roughness values have a significant impact on the wear mechanism of composite materials[47]. Figure 15. depicts the mean surface roughness qualities of composite materials before and after experiments (at 50 N, and 5 m/s). Regarding the test, the surface quality of the treated fiber composites (A1, B2, C3, and D4) escalated dramatically. This demonstrates that the A1, B2, C3, and D4 fiber composite samples deteriorated with significant damage during the sliding test due to poor bond formation between both the high weight percentage of Juliflora bark powder and the polyester matrix. The coarse texture of its exterior increased the wear rate. Lower roughness values were observed for treated fiber-reinforced samples due to less sample destruction at the contact surface due to good interfacial bonding. The hybrid composites with 40% kenaf treated fiber (E5) had the lowest roughness value of the composite materials studied (0.066 mm).

5. Conclusions

The tribological performance and DMA of NF (jute, kenaf, and Juliflora bark powder) reinforced polyester blends were evaluated in the current study, and SEM was used to analyse the geomorphology of damaged samples, indicating out surfaces. The current findings lead to the following conclusions:

- At elevated speeds, the effect of speed on the frictional coefficient is minimal, whilst the influence of applied load on the frictional coefficient is the least. The developed composite's wear performance is significantly impacted by sliding speed in addition to the applied stresses.
- At a higher load of 50N, the wear rate percentage of hybrid composite samples such as A1, B2, C3, and D4 achieved 69.13%, 59.58, 44.26%, and 22.56% respectively compared with the E5 sample.
- The visco-elastic characteristics of the manufactured composites had high storage modulus (4.1 GPa) and loss modulus (3.8 GPA). According to the results of damping capability tests, the addition of natural

fibers significantly reduced the brittleness of the polyester matrix.
- Failure mechanisms such as cracks, fiber matrix cracking, and matrix debonding were visible in SEM images.
- These composite materials can be used for a variety of industrial purposes in the automotive, industrial, and civil sectors.

6. References

1. Cripps A, Harris B, Ibell T. C564 Fiber-reinforced polymer composites in construction. London: CIRIA; 2002.
2. Karimah A, Ridho MR, Munawar SS, Adi DS, Damayanti R, Subiyanto B, et al. A review on natural fibers for development of eco-friendly bio-composite: characteristics, and utilizations. J Mater Res Technol. 2021;79:2442-58.
3. Yingji W, Cai L, Mei C, Lam S, Su CS, Shi SQ, et al. Development and evaluation of zinc oxide-blended kenaf fiber biocomposite for automotive applications. Mater Today Commun. 2020;24:101008.
4. Manalo A, Aravinthan T, Karunasena W, Ticoalu A. A review of alternative materials for replacing existing timber sleepers. Compos Struct. 2010;92:603-11.
5. Chang BP, Chan WH, Zamri MH, Akil HM, Chuah HG. Investigating the effects of operational factors on wear properties of heat-treated pultruded kenaf fiber-reinforced polyester composites using taguchi method. J Nat Fibers. 2019;16:702-17.
6. Sudhagar, S, Kumar, SS, Premkumar, IJI, Vijayan, V, Venkatesh, R, Rajkumar, S, et al. UV and visiblelightdriven TiO_2/La_2O_3 and TiO_2/Al_2O_3 nano catalysts: synthesis and enhanced photocatalytic activity. Appl Phys, A Mater Sci Process. 2002;128:1-16.
7. Ahmadian R, Mantena PR. Modal characteristics of structural portal frames made of mechanically joined pultruded flat hybrid composites. Compos, Part B Eng. 1996;27:319-28.
8. Alves C, Silva AJ, Reis LG, Freitas M, Rodrigues LB, Alves DE. Ecodesign of automotive components making use of natural jute fiber composites. J Clean Prod. 2010;18:313-27.
9. Holbery J, Houston D. Natural-fiber-reinforced polymer composites in automotive applications. JOM. 2006;58:80-6.
10. Ouarhim W, Essabir H, Bensalah MO, Rodrigue D, Bouhfid R, Qaiss AEQ. Hybrid composites and intra-ply hybrid composites based on jute and glass fibers: a comparative study on moisture absorption and mechanical properties. Mater Today Commun. 2020;22:100861.
11. Bajpai PK, Singh I, Madaan J. Tribological behavior of natural fiber reinforced PLA composites. Wear. 2013;297:829-40.
12. Barbero J. Ever, introduction to composite materials design. Boca Raton: CRC Press; 2010.
13. Yousif BF, El-Tayeb NSM. Wear and friction characteristics of CGRP composite under wet contact condition using two different test techniques. Wear. 2008;265:856-64.
14. Borruto A, Crivellone G, Marani F. Influence of surface wettability on friction and wear tests. Wear. 1998;222:57-65.
15. Prasob PA, Sasikumar M. Viscoelastic and mechanical behaviour of reduced graphene oxide and zirconium dioxide filled jute/epoxy composites at different temperature conditions. Mater Today Commun. 2019;19:252-61.
16. Wu J, Cheng XH. The tribological properties of Kevlar pulp reinforced epoxy composites under dry sliding and water lubricated condition. Wear. 2006;261:1293-7.
17. Sathees Kumar S. Dataset on mechanical properties of natural fiber reinforced polyester composites for engineering applications. Data Brief. 2020;30:105054.
18. Bajpai PK, Singh I, Madaan J. Frictional and adhesive wear performance of natural fibre reinforced polypropylene composites. Proceedings of the Institution of Mechanical Engineers, Part J: Journal of Engineering Tribology. 2013;227(4);385-392.
19. Sathees Kumar S, Mugesh Raja V, Nithin Chakravarthy CH, Muthalagu R. Determination of mechanical properties and characterization of alkali treated sugarcane bagasse, pine apple leaf and sisal fibers reinforced hybrid polyester composites for various applications. Fibers Polym. 2021;22:1675-83.
20. Sathees Kumar S, Mugesh Raja V. Processing and determination of mechanical properties of prosopisjuliflora bark, banana and coconut fiber reinforced hybrid bio composites for an engineering field. Compos Sci Technol. 2021;208:108695.
21. Van de Weyenberg I, Chi Truong T, Vangrimde B, Verpoest I. Improving the properties of UD flax fiber reinforced composites by applying an alkaline fiber treatment. Compos, Part A Appl Sci Manuf. 2006;37:1368-76.
22. Chin CW, Yousif BF. Potential of kenaf fibers as reinforcement for tribological applications. Wear. 2009;267:1550-7.
23. Heckadka SS, Suhas Yeshwant N, Sathish R, Rashmi S, Shrinidhi LK, Krishna MS. Two body wear characteristics of polyalthia longifolia/mangifera indica/jute fiber reinforced epoxy composites using taguchi technique. Mater Res. 2021;24:1-13.
24. El-Tayeb, NSM. A study on the potential of sugarcane fibers/polyester composite for Tribological applications. Wear. 2008;265(1-2):223-35.
25. Yousif BF, Chin CW. Epoxy composite based on kenaf fibers for tribological applications under wet contact conditions. Surf Rev Lett. 2012;19:1250050.
26. Mohanty S, Verma SK, Nayak SK. Dynamic mechanical and thermal properties of MAPE treated jute/HDPE composites. Compos Sci Technol. 2006;66:538-47.
27. Muthalagu R, Srinivasan V, Sathees Kumar S, Murali Krishna V. Extraction and effects of mechanical characterization and thermal attributes of Jute, Prosopis juliflora bark and Kenaf fibers reinforced bio composites used for engineering applications. Fibers Polym. 2021;22:2018-26.
28. Chaudhary, V, Pramendra KB, Sachin M. An investigation on wear and dynamic mechanical behavior of jute/hemp/flax reinforced composites and its hybrids for tribological applications. Fibers Polym. 2018;19:403-15.
29. Dwivedi UK, Chand N. Influence of MA-g-PP on abrasive wear behaviour of chopped sisal fiber reinforced polypropylene composites. J Mater Process Technol. 2009;209:5371-5.
30. Chand N, Dwivedi UK. Effect of coupling agent on abrasive wear behaviour of chopped jute fiber-reinforced polypropylene composites. Wear. 2006;261:1057-63.
31. Agrawal S, Singh KK, Sarkar PK. A comparative study of wear and friction characteristics of glass fiber reinforced epoxy resin, sliding under dry, oil-lubricated and inert gas environments. Tribol Int. 2016;96:217-24.
32. Sudhagar S, Sathees Kumar S, Isaac Premkumar IJ, Vijayan V, Venkatesh R, Rajkumar S, et al. UV- and visible-light-driven TiO2/La2O3 and TiO2/Al2O3nanocatalysts: synthesis and enhanced photocatalytic activity. Appl Phys, A Mater Sci Process. 2022;128:1-16.
33. Alajmi M, Shalwan A. Correlation between mechanical properties with specific wear rate and the coefficient of friction of graphite/epoxy composites. Materials (Basel). 2015;8:4162-75.
34. Mugesh Raja V, Sathees Kumar S. Exploration of mechanical attributes, thermal behaviors and atomic force analysis of alkali treated hybrid polyester composites for an engineering application. Fibers Polym. 2021;22:2535-42.
35. Saba N, Jawaid M, Alothman OY, Paridah MT. A review on dynamic mechanical properties of natural fiber reinforced polymer composites. Constr Build Mater. 2016;106:149-59.
36. Gupta, MK, Ajaya B. Natural fiber reinforced polymer composites: a review on dynamic mechanical properties. Curr Trends Fashion Technol Textile Eng. 2017;1(3):55-8.

37. Huda MS, Drzal LT, Mohanty AK, Misra M. Effect of fiber surface-treatments on the properties of laminated biocomposites from poly(lactic acid) (PLA) and kenaf fibers. Compos Sci Technol. 2008;68(2):424-32.
38. Costa CSMF, Fonseca AC, Serra AC, Coelho JFJ. Dynamic mechanical thermal analysis of polymer composites reinforced with natural fibers. Polym Rev (Phila Pa). 2014;56:362-83.
39. Sundararajan G, Roy M, Venkataraman B. Erosion efficiency-a new parameter to characterize the dominant erosion micro mechanism. Wear. 1990;40:369-81.
40. Sathees Kumar S, Vishnu Vardhan T, Sridhar Babu B, Nithin Chakravarthy CH, Prabhakar N, Venkateswar Rao K, et al. Dataset on tribological, characterization and thermal properties of Silicon carbide reinforced polyamide composites for industrial applications. Data Brief. 2020;30:105662.
41. Mohanty AK, Tummala P, Liu W, Misra M, Mulukutla PV, Drzal LT. Injection molded biocomposites from soy protein based bioplastic and short industrial hemp fiber. J Polym Environ. 2005;13:279-285.
42. Arun Raja AK, Arun Vasantha Geethan K, Sathees Kumar S, Sabarish Kumar P. Influence of mechanical attributes, water absorption, heat deflection features and characterization of natural fibers reinforced epoxy hybrid composites for an engineering application. Fibers Polym. 2021;22:3444-55.
43. Sathees Kumar S. Effect of natural fiber loading on mechanical properties and thermal characteristics of hybrid polyester composites for industrial and construction fields. Fibers Polym. 2020;21:1508-14.
44. Viswanath SB, Sathees Kumar S Sudarsan D, Muthalagu R. Mechanical attributes of coir fiber, rice husk and egg shell reinforced hybrid polyester composites. Mater Today: Proc. 46(Pt 1):874-7.
45. Gerard VE, Cattell C, Ayers S. A fair dinkum approach to fiber composites in civil engineering. Constr Build Mater. 2006;20:2-10.
46. Nak-Ho S, Suh NP. Effect of fiber orientation on friction and wear of fiber reinforced polymeric composites. Wear. 1979;53:129-41.
47. Satheeskumar S, Kanagaraj G. Experimental investigation on tribological behaviours of PA6, PA6-reinforced Al2 O 3 and PA6-reinforced graphite polymer composites. Bull Mater Sci. 2016;39:1467-81.